Photochemically driven redox chemistry induces protocell membrane pearling and division

Ting F. Zhu, Katarzyna Adamala, Na Zhang, and Jack W. Szostak[1]

Department of Molecular Biology, and Center for Computational and Integrative Biology, Howard Hughes Medical Institute, Massachusetts General Hospital, Boston, MA 02114

Edited by* Gerald F. Joyce, The Scripps Research Institute, La Jolla, CA, and approved May 10, 2012 (received for review February 26, 2012)

Prior to the evolution of complex biochemical machinery, the growth and division of simple primitive cells (protocells) must have been driven by environmental factors. We have previously demonstrated two pathways for fatty acid vesicle growth in which initially spherical vesicles grow into long filamentous vesicles; division is then mediated by fluid shear forces. Here we describe a different pathway for division that is independent of external mechanical forces. We show that the illumination of filamentous fatty acid vesicles containing either a fluorescent dye in the encapsulated aqueous phase, or hydroxypyrene in the membrane, rapidly induces pearling and subsequent division in the presence of thiols. The mechanism of this photochemically driven pathway most likely involves the generation of reactive oxygen species, which oxidize thiols to disulfide-containing compounds that associate with fatty acid membranes, inducing a change in surface tension and causing pearling and subsequent division. This vesicle division pathway provides an alternative route for the emergence of early self-replicating cell-like structures, particularly in thiol-rich surface environments where UV-absorbing polycyclic aromatic hydrocarbons (PAHs) could have facilitated protocell division. The subsequent evolution of cellular metabolic processes controlling the thiol:disulfide redox state would have enabled autonomous cellular control of the timing of cell division, a major step in the origin of cellular life.

origin of life | vesicles

One model for the nature of the earliest and simplest cells, or protocells, is that they consisted of a self-replicating membrane compartment (vesicle) that encapsulated a self-replicating genetic polymer (1). The emergence of any genetically encoded function that enhanced protocell reproduction or survival would have marked the beginnings of Darwinian evolution and, thus, of biology itself. We have been attempting to test various aspects of this model for the origin of cellular life through the laboratory construction and characterization of model protocells (2, 3). A necessary and complementary aspect of this program is the exploration of environmental scenarios in which external inputs of matter and energy could drive the replication of the genetic material of a protocell (4), as well as protocell membrane growth and division (5, 6). For example, we recently showed that activated nucleotides, added to a suspension of model protocells, could cross the vesicle membrane and copy encapsulated nucleic acid templates (4). We have also shown that large multilamellar fatty acid vesicles can grow by absorbing fatty acid molecules from added fatty acid micelles (6). This growth pathway begins with the emergence of a thin membranous filament from the side of the initially spherical vesicle; the filament grows and gradually incorporates the contents and membranes of the parent vesicle, which is transformed into a long filamentous vesicle. Under modest shear forces, the filamentous vesicle divides into multiple daughter vesicles (6). The emergence of more robust forms of cellular life requires mechanisms that can drive growth and division independently of environmental perturbations. As a potential example, we recently showed that fatty acid vesicles that contain a small proportion of phospholipids can grow into filamentous vesicles by absorbing fatty acid molecules from neighbouring vesicles that lack phospholipids (2). Thus, the evolution of an internal metabolic pathway for phospholipid synthesis could drive the growth of a primitive cell in such a manner as to be predisposed for division in response to environmental fluid shear forces.

While the spontaneous division of model protocells occurs readily after growth as a result of environmental shear forces, this process is not readily amenable to evolutionary modification into an internally controllable process. Here we describe an alternative process for protocell division based on simple chemical and physical mechanisms. Because this process is based upon a change in the redox state of small thiol containing molecules, the evolution of an internal redox metabolism would allow cells to control the timing of their cell division independently of environmental fluctuations.

Results

During the course of our imaging studies of vesicle growth and division, we observed an unexpected artifact: Long thread-like oleate vesicles containing an encapsulated fluorescent dye quickly (in approximately 5 s) round up into large spherical vesicles under intense illumination (Fig. S1 and Movie S1). The vesicles contained 2 mM HPTS (8-hydroxypyrene-1,3,6-trisulfonic acid trisodium salt, a water-soluble, membrane-impermeable fluorescent dye) (7) and were illuminated by an EXFO 120 W metal halide lamp. We reasoned that since most fluorescent dyes, such as HPTS, generate reactive oxygen species (ROS) under illumination, this phenomenon might be caused by the radical-mediated oxidation and fragmentation of the internal buffer solute, bicine, leading to increased internal osmolarity, as previously seen in the case of spherical vesicles that explode under similar conditions (8). The fact that the sphere-to-filament transition is reversible shows directly that growth into a filamentous form does not involve topological changes in vesicle structure. In an effort to obtain better images of filamentous vesicles, we added 10 mM dithiothreitol (DTT) to a vesicle suspension to scavenge ROS, in an attempt to block the rounding-up artifact. To our surprise, intense illumination in the presence of 10 mM DTT caused the thread-like fatty acid vesicles to go through pearling and subsequent division (Fig. 1 and Movie S2). The long thread-like membrane first transformed into a periodic string of smaller ellipsoidal vesicles connected by narrow necks, and the smaller vesicles eventually separated into independent vesicles that moved apart by Brownian motion.

Author contributions: T.F.Z., K.A., N.Z., and J.W.S. designed research; T.F.Z., K.A., and N.Z. performed research; T.F.Z., K.A., N.Z., and J.W.S. analyzed data; and T.F.Z. and J.W.S. wrote the paper.

The authors declare no conflict of interest.

*This Direct Submission article had a prearranged editor.

Freely available online through the PNAS open access option.

[1]To whom correspondence should be addressed. E-mail: szostak@molbio.mgh.harvard.edu.

This article contains supporting information online at www.pnas.org/lookup/suppl/doi:10.1073/pnas.1203212109/-/DCSupplemental.

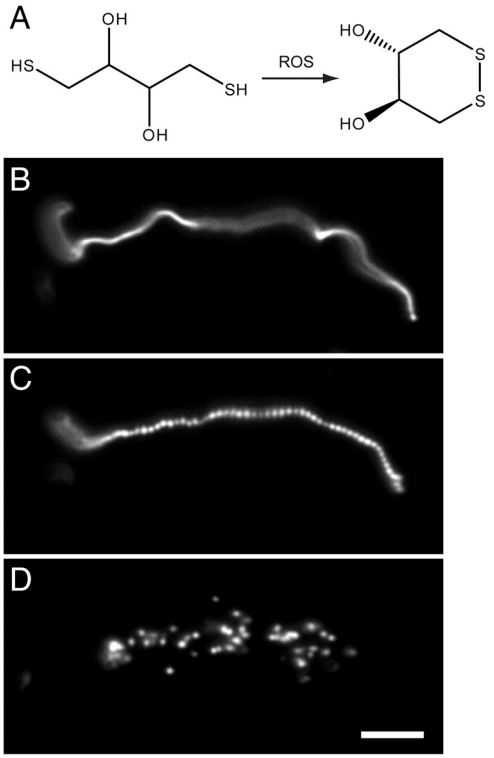

Fig. 1. Oleate vesicle pearling and division. (*A*) Radical-mediated oxidation of DTT. (*B*) An oleate vesicle (containing 2 mM HPTS, in 0.2 M Na-glycinamide, pH 8.5, 10 mM DTT) 30 min after the addition of five equivalents of oleate micelles. (*C* and *D*) Under intense illumination (for 2 s and 12 s, respectively), the long thread-like vesicle went through pearling and division (Movie S2). Scale bar, 10 μm.

We also show that the pearling and division can happen not only in fully grown, filamentous vesicles, but also at intermediate growth stages. We have previously shown that oleate vesicles, when fed with small quantities of micelles (one equivalent), can transform into sphere-tail shapes and divide under gentle fluid shear forces (6). We tested whether the addition of DTT could cause oleate vesicles at sphere-tail stages (containing 2 mM HPTS, in 0.2 M Na-bicine, pH 8.5, 30 min after the addition of one equivalent of oleate micelles) to divide without requiring external mechanical forces. With 10 mM DTT in the solution and under intense illumination, pearling and division of the filamentous portions of vesicles were indeed observed (Fig. S2 *A* and *B*; Movies S3 and S4).

To understand the mechanisms responsible for the pearling and division of thread-like fatty acid vesicles, we examined oleate vesicles labeled with different dyes, in either the internal aqueous space or in the membrane itself. When we prepared vesicles containing 2 mM calcein (bis[*N*,*N*-bis(carboxymethyl)aminomethyl] fluorescein) in the internal aqueous space and added 10 mM DTT 30 min after the addition of five equivalents of oleate micelles, vesicle pearling and division were again observed upon illumination. In contrast, we found that long thread-like oleate vesicles labeled with a low concentration of membrane-localized dye [0.5 mol% Rh-DHPE (Lissamine rhodamine B 1,2-dihexadecanoyl-*sn*-glycero-3-phosphoethanolamine)] did not go through pearling and division (Fig. S3 *A* and *B*). This may be because there are fewer dye molecules associated with the vesicles in the latter case, since in a control experiment where the encapsulated water-soluble fluorescent dye was adjusted to a lower concentration (0.05 mM) comparable to that of the membrane dye used, no vesicle pearling and division were observed. We also observed that with equal concentrations (2 mM) of HPTS inside and outside of the filamentous vesicles (labeled with 1 mol% Rh-DHPE for imaging), vesicle pearling and division still occurred (Fig. S4). This result indicates that a cross-membrane concentration gradient of the fluorescent dye is not a prerequisite for the pearling and division phenomenon.

It has been shown that vesicle pearling and division can occur as a result of laser tweezers induced surface tension changes which induce a Rayleigh instability in vesicle membranes (9). Recent experiments have also shown that encapsulated cationic nanoparticles can induce vesicle pearling (10). We hypothesized that the photochemically induced oxidation of thiols into its oxidized form, *trans*-4,5-dihydroxy-1,2-dithiane, resulted in an increased hydrophobicity of the compound (logP 0.12 for DTT vs. logP 0.52 for *trans*-4,5-dihydroxy-1,2-dithiane), and consequently increased interaction of the molecule with the membrane. We used NMR methods to examine the interaction of DTT and its oxidation product with fatty acid vesicle membranes. Because the proton chemical shifts of both DTT and *trans*-4,5-dihydroxy-1,2-dithiane overlap with the strong background peaks of bicine buffer at 2–4 ppm (and other organic buffers such as tricine and TRIS), which are difficult to selectively suppress, we used oleate vesicles prepared without buffer (15 mM oleate in 7.5 mM NaOD solution in D_2O, pD approximately 8.5) for the following experiments. We added 15 mM DTT and 15 mM *trans*-4,5-dihydroxy-1,2-dithiane to vesicles prepared as above and used two independent NMR methods to examine the interaction of these small molecules with the oleate membranes. We first used saturation transfer difference (STD) spectroscopy, a widely used method for examining the interaction of small ligands with large receptors (11, 12). Following selective saturation irradiation of the oleate vinyl protons, we observed saturation transfer to the CH protons of *trans*-4,5-dihydroxy-1,2-dithiane but not to the CH protons of DTT (Fig. 2 *A* and *B*). Thus, only the oxidized form of DTT appears to interact with oleate membranes. As a further test, we used the waterLOGSY method, another sensitive NMR method commonly used for screening ligand-receptor interactions (13). Again, only oxidized and not reduced DTT was observed to interact with the oleate bilayer membrane (Fig. 2*C*).

We have shown that fatty acid vesicles of other lipid compositions, such as decanoate:decanol (2:1), can grow into filamentous vesicles when fed with two equivalents of decanoate micelles and one equivalent of decanol emulsion (6). With 10 mM DTT in the solution, intense illumination of decanoate:decanol (2:1) vesicles containing 2 mM HPTS led to pearling and division (Fig. S2 *C* and *D*). Since both decanoic acid and decanol have saturated hydrocarbon chains that are unlikely to react with ROS or DTT, this experiment suggests that oxidation of the carbon-carbon double bond in fatty acids is unlikely to be the cause of vesicle pearling. We also tested whether phospholipid vesicles can go through pearling and division with DTT in the solution. We found that POPC (1-palmitoyl-2-oleoyl-*sn*-glycero-3-phosphocholine) vesicles containing 2 mM HPTS, after the addition of 0.5 M sucrose (to produce thread-like vesicles by osmotically driven water efflux) and under intense illumination, did not go through pearling and division (Fig. S3 *C* and *D*), presumably due to less dramatic changes in the membrane surface tension in phospholipid vesicles.

To further understand the effect of thiols on vesicle pearling and division, we asked whether other thiols can also cause this phenomenon. Thiols, such as 3-mercaptopropionic acid (10 mM), 3-mercapto-1-propanol (50 mM), 1-mercapto-2-propanol (50 mM), and 3-mercapto-1,2,4-triazole (50 mM), all caused thread-like oleate vesicles containing 2 mM HPTS to undergo pearling and division (Fig. 3). At lower thiol concentrations (2 mM 3-mercaptopropionic acid, 10 mM 3-mercapto-1-propanol, 10 mM 1-mercapto-2-propanol, and 10 mM 3-mercapto-1,2,4-triazole), vesicle pearling was observed but without subsequent division. Recent evidence suggests that the thiol-containing amino acid cysteine may have been prebiotically available, as

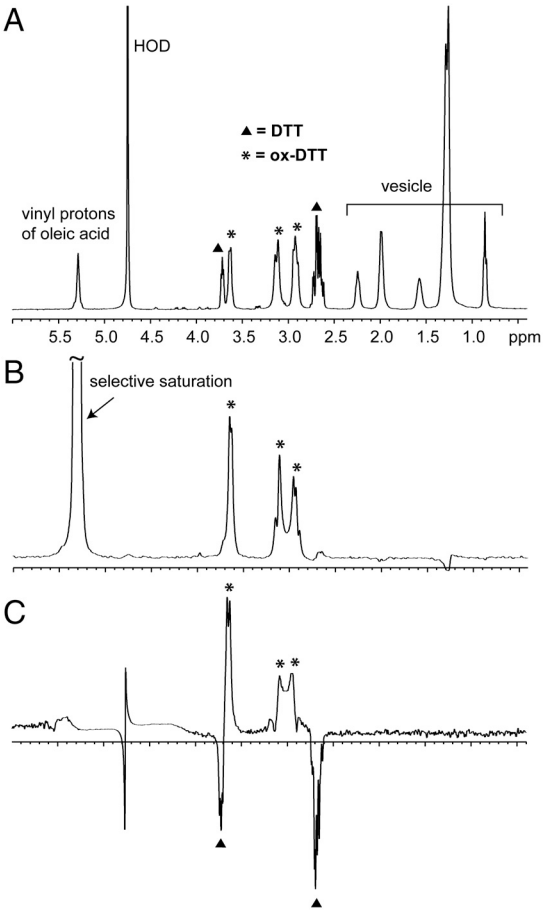

Fig. 2. NMR experiments to characterize the association of oxidized but not reduced DTT with oleate bilayer membranes. (*A*) Reference spectrum: conventional 1D ^{1}H spectrum of oleic acid vesicles (15 mM oleate, 7.5 mM NaOD in 100% D_2O, pH approximately 8.5), with 15 mM DTT and 15 mM *trans*-4,5-dihydroxy-1,2-dithiane added. Peaks corresponding to DTT (solid triangles) and its oxidized form *trans*-4,5-dihydroxy-1,2-dithiane (ox-DTT; stars) were assigned by spiking with the two compounds respectively. (*B*) STD (saturation transfer difference) spectrum of the above mixture in 100% D_2O. The vinyl protons of oleic acid were selectively irradiated. Positive peaks reveal the interaction of *trans*-4,5-dihydroxy-1,2-dithiane molecules with oleate molecules of the bilayer membrane (stars). The absence of detectable peaks for DTT molecules suggests that DTT does not interact significantly with the oleate membranes. (*C*) WaterLOGSY (water ligand observed via gradient spectroscopy) spectrum of the above mixture in 10% D_2O. Positive peaks show the interaction of oxidized DTT molecules with the oleate bilayer membranes (stars), while negative peaks suggest the absence of DTT association with bilayer membranes (solid triangles).

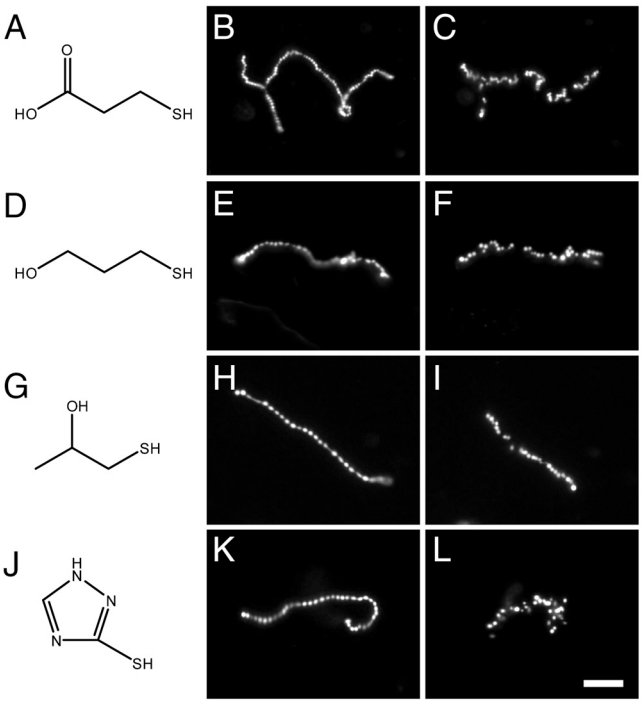

Fig. 3. Oleate vesicle pearling and division with various thiols in the solution. (*A*) 3-mercaptopropionic acid. (*B* and *C*) An oleate vesicle (containing 2 mM HPTS, in 0.2 M Na-bicine, pH 8.5, 10 mM 3-mercaptopropionic acid, 30 min after the addition of five equivalents of oleate micelles) went through pearling and division under intense illumination (for 3 s and 15 s, respectively). (*D*) 3-mercapto-1-propanol. (*E* and *F*) An oleate vesicle as above but in 50 mM 3-mercapto-1-propanol, went through pearling and division under intense illumination (for 2 s and 10 s, respectively). (*G*) 1-mercapto-2-propanol. (*H* and *I*) An oleate vesicle as above but in 50 mM 1-mercapto-2-propanol went through pearling and division under intense illumination (for 2 s and 9 s, respectively). (*J*) 3-mercapto-1,2,4-triazole. (*K* and *L*) An oleate vesicle as above but in 50 mM 3-mercapto-1,2,4-triazole went through pearling and division under intense illumination (for 3 s and 13 s, respectively). Scale bar, 20 μm.

cysteine oxidation products have been found in the material from a 1958 Miller H_2S-rich spark discharge experiment (14). When we tested cysteine, we observed vesicle pearling but not division. We then considered the possibility that the cys-cys dipeptide, di-L-cysteine (15), might allow pearling and division of vesicles after oxidation to generate an intramolecular disulfide bond. When we prepared filamentous oleate vesicles containing 20 mM di-L-cysteine and 2 mM HPTS in the internal aqueous phase, we observed both vesicle pearling and division upon illumination (Fig. 4).

As an initial step toward exploring prebiotically plausible scenarios in which photochemically driven pearling and division might operate, we tested the idea that polycyclic aromatic hydrocarbons (PAHs) might replace the synthetic fluorescent dyes used in the above experiments (16). PAHs are the most abundant polyatomic organic molecules in the universe, have been postulated to play important roles in the origin of life (16, 17), and have been shown to stabilize short-chain fatty acid membranes (18). We therefore asked whether oxygenated derivatives of PAHs, such as 1-hydroxypyrene (while HPTS itself is also a hydroxypyrene derivative, it is unlikely to be prebiotically abundant), can be incorporated into vesicle membranes and act as photosensitizers that can absorb UV radiation, generate ROS, and facilitate the division of protocells. To test this idea experimentally, we dissolved a high concentration of 1-hydroxypyrene (20 mol%), oleic acid and a low concentration of Rh-DHPE (1 mol% for imaging) in a chloroform solution, followed by rotary evaporation and resuspension in buffer (0.2 M Na-bicine, pH 8.5). After vesicle growth into filamentous form, and in the presence of 15 mM DTT and UV illumination, vesicle pearling and division were indeed observed (Fig. 5 and Movie S5).

Discussion

Our observations strongly suggest that oxidized, but not reduced, thiols can associate with membranes, triggering division in our protocell model. While the mechanism by which disulfide-containing compounds cause membrane pearling and division is not entirely clear, it is plausible that disulfide-membrane interactions lead to changes in surface tension. Changes in membrane surface tension due to externally applied force from optical tweezers have been shown to induce pearling in tubular vesicles (9, 19), as well as vesicle expulsion (20). Vesicle pearling has also been demonstrated by insertion of amphiphilic polymers in the outer leaflet of the membrane, inducing changes in spontaneous curvature (21, 22). In addition, lipid phase separation has been

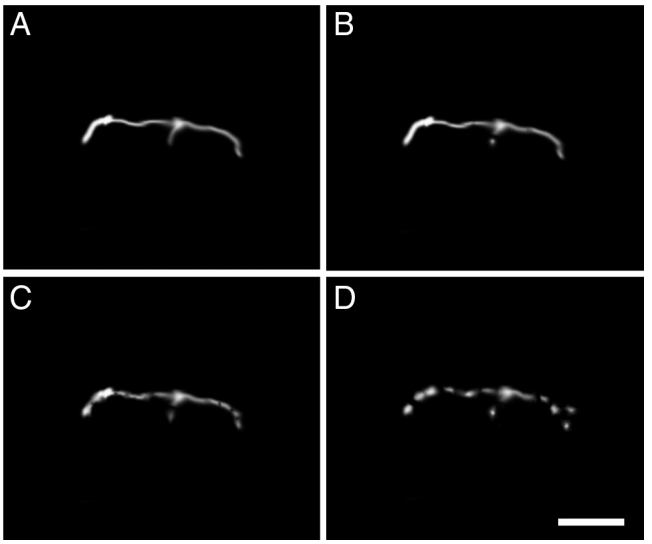

Fig. 4. Oleate vesicle pearling and division mediated by the dipeptide di-L-cysteine. (*A*) An oleate vesicle (containing 2 mM HPTS, in 0.2 M Na-bicine, pH 8.5, 20 mM di-L-cysteine) 30 min after the addition of five equivalents of oleate micelles. (*B–D*) Under intense illumination (for 3 s, 8 s, and 12 s, respectively), the long thread-like vesicle went through pearling and division. Scale bar, 10 μm.

shown to drive vesicle budding and division as a consequence of minimizing interdomain edge energy (23). While our results suggest that the oxidation of dithiothreitol to *trans*-4,5-dihydroxy-1,2-dithiane results in increased interaction of the molecule with the membrane, how such interactions lead to membrane pearling and division remains unclear. Future studies will be required to investigate the location and homogeneity or heterogeneity of disulfide association with the bilayer membrane in order to quantitatively understand the resulting changes in morphology of the vesicle membrane.

The observation that thiols and UV-absorbing PAHs facilitate vesicle pearling and division may have important implications for understanding the origin of cellular life. Thiols are likely to have been abundant in prebiotic hydrothermal systems, such as near-surface hydrothermal vents (24). Oxygenated PAH fragments could be generated by hydrothermal processing of meteoritic kerogen or by pyrolysis of organic materials. Such hydrophobic molecules are likely to have been selectively solubilized and concentrated in primitive membranes. Indeed, hydroxypyrene, a simple oxygenated PAH, has been shown to integrate into and stabilize membranes composed of short chain fatty acids (18). In a high UV surface environment, membrane-localized PAHs would be expected to absorb UV radiation and generate ROS, even under anaerobic conditions (16). Our observations show that in the presence of thiols, generation of ROS could lead to the pearling and subsequent division of filamentous vesicles composed of fatty acids and PAHs, thus providing an independent pathway for protocell division that is distinct from the previously described shear force-dependent pathway (6).

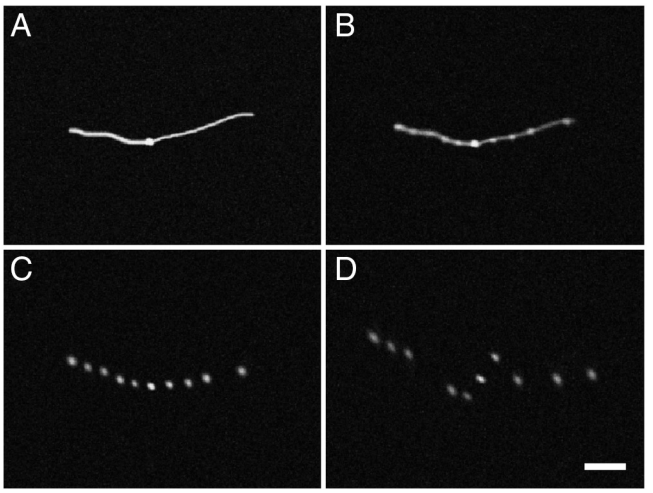

Fig. 5. Pearling and division of an oleate vesicle containing 1-hydroxypyrene in the membrane. (*A*) An oleate vesicle (with 20 mol%1-hydroxypyrene and 1 mol% Rh-DHPE in the membrane, in 0.2 M Na-bicine, pH 8.5, 15 mM DTT) 30 min after the addition of five equivalents of oleate micelles. (*B–D*) Under intense illumination (for 57 s, 153 s, and 213 s, respectively), the long thread-like vesicle went through pearling and division (Movie S5). Scale bar, 10 μm.

The control of the timing of cell division by thiol redox state provides a mechanism by which an initial dependence on environmental fluctuations could transition to an internally controlled process, through the evolution of cellular metabolism. For example, we have shown that the dipeptide cys–cys can result in vesicle pearling and division, whereas the amino acid cysteine by itself cannot. Therefore, metabolic control of dipeptide synthesis and degradation could potentially mediate the control of the timing of cell division in primitive cells. Alternatively, as cellular metabolism evolved to the point that cells derived energy from environmental redox disequilibrium, they could potentially use the control of their internal thiol:disulfide redox state as a means of controlling cell division. Finally, it would be interesting to investigate the possibility that intracellularly produced small molecules, peptides, or structured RNAs that interact with protocell membranes might also lead to pearling and division. Such processes would result in competition between protocells on the basis of faster or more appropriately timed cell division, and thus control of cell size, foreshadowing the rise of more complex and more tightly regulated modes of cell division.

Materials and Methods

Vesicle Preparation. Oleate vesicles were prepared by resuspending a dried film of oleic acid (Nu-Chek Prep) in 0.2 M Na-bicine (Sigma-Aldrich) containing 2 mM HPTS at pH 8.5, to a final concentration of 10 mM oleic acid. Large (approximately 4 μm in diameter) monodisperse multilamellar vesicles were prepared by extrusion and large-pore dialysis as described (7). Oleate vesicles containing 1-hydroxypyrene (Sigma-Aldrich) in the membrane were prepared by co-dissolving 1-hydroxypyrene (20 mol%), oleic acid, and Rh-DHPE (1 mol%) in a chloroform solution, followed by rotary evaporation and resuspension in buffer (0.2 M Na-bicine, pH 8.5, 15 mM DTT). Oleate vesicles containing di-L-cysteine were prepared by resuspension of 10 mM oleic acid in 0.2 M Na-bicine (pH 8.5) containing 2 mM HPTS and 20 mM di-L-cysteine. Di-L-cysteine (cysteinylcysteine) was prepared using F-moc solid phase synthesis on a microwave peptide synthesizer as described (15).

Imaging Vesicle Pearling and Division. Vesicle growth experiments were performed as described (6), in a buffer solution containing DTT, 3-mercaptopropionic acid, 3-mercapto-1-propanol, 1-mercapto-2-propanol, 3-mercapto-1,2,4-triazole, or di-L-cysteine. Vesicle pearling and division were imaged using a Nikon TE2000S inverted epifluorescence microscope with extra-long working distance (ELWD) objective lenses (Nikon). The illumination source was a metal halide lamp (EXFO) with a 480 ± 20 nm (for HPTS), 546 ± 5 nm (for Rh-DHPE), or 360 ± 20 nm (for UV) optical filter (Chroma).

NMR Measurements. All NMR spectra were recorded at 293 K with a Varian 400 MHz NMR spectrometer (Oxford AS-400) equipped with a 5 mm broadband PFG (z-gradient) probe. DTT and *trans*-4,5-dihydroxy-1,2-dithiane (Sigma-Aldrich) at concentrations of 15–20 mM were added to sonicated vesicle suspensions prior to NMR measurements. Oleate vesicles were prepared without buffer by mixing 15 mM oleate with 7.5 mM NaOD (pH approximately 8.5, in 100% D_2O for STD experiments and in 10% D_2O for waterLOGSY experiments).

ACKNOWLEDGMENTS. We thank R. Bruckner, I. Budin, I. Chen, C. Hentrich, and S. Mansy for discussions and comments on the manuscript. J.W.S. is an investigator of the Howard Hughes Medical Institute. This work was supported in part by grant EXB02-0031-0018 from the NASA Exobiology Program to J.W.S.

1. Szostak JW, Bartel DP, Luisi PL (2001) Synthesizing life. *Nature* 409:387–390.
2. Budin I, Szostak JW (2011) Physical effects underlying the transition from primitive to modern cell membranes. *Proc Natl Acad Sci USA* 108:5249–5254.
3. Chen IA, Roberts RW, Szostak JW (2004) The emergence of competition between model protocells. *Science* 305:1474–1476.
4. Mansy SS, et al. (2008) Template-directed synthesis of a genetic polymer in a model protocell. *Nature* 454:122–125.
5. Hanczyc MM, Fujikawa SM, Szostak JW (2003) Experimental models of primitive cellular compartments: Encapsulation, growth, and division. *Science* 302:618–622.
6. Zhu TF, Szostak JW (2009) Coupled growth and division of model protocell membranes. *J Am Chem Soc* 131:5705–5713.
7. Zhu TF, Szostak JW (2009) Preparation of large monodisperse vesicles. *PLoS ONE* 4:e5009.
8. Zhu TF, Szostak JW (2011) Exploding vesicles. *J Syst Chem* 2:4.
9. Bar-Ziv R, Moses E (1994) Instability and "pearling" states produced in tubular membranes by competition of curvature and tension. *Phys Rev Lett* 73:1392–1395.
10. Yu Y, Granick S (2009) Pearling of lipid vesicles induced by nanoparticles. *J Am Chem Soc* 131:14158–14159.
11. Haselhorst T, Lamerz AC, Itzstein M (2009) Saturation transfer difference NMR spectroscopy as a technique to investigate protein-carbohydrate interactions in solution. *Methods Mol Biol* 534:375–386.
12. Mayer M, Meyer B (2001) Group epitope mapping by saturation transfer difference NMR to identify segments of a ligand in direct contact with a protein receptor. *J Am Chem Soc* 123:6108–6117.
13. Dalvit C, Fogliatto G, Stewart A, Veronesi M, Stockman B (2001) WaterLOGSY as a method for primary NMR screening: Practical aspects and range of applicability. *J Biomol NMR* 21:349–359.
14. Parker ET, et al. (2011) Primordial synthesis of amines and amino acids in a 1958 Miller H2S-rich spark discharge experiment. *Proc Natl Acad Sci USA* 108:5526–5531.
15. Erdelyi M, Gogoll A (2002) Rapid microwave-assisted solid phase peptide synthesis. *Synthesis-Stuttgart* 11:1592–1596.
16. Deamer DW (1992) Polycyclic aromatic hydrocarbons: Primitive pigment systems in the prebiotic environment. *Adv Space Res* 12:183–189.
17. Ehrenfreund P, Rasmussen S, Cleaves J, Chen L (2006) Experimentally tracing the key steps in the origin of life: The aromatic world. *Astrobiology* 6:490–520.
18. Cape JL, Monnard PA, Boncella JM (2011) Prebiotically relevant mixed fatty acid vesicles support anionic solute encapsulation and photochemically catalyzed transmembrane charge transport. *Chem Sci* 2:661–671.
19. Nelson P, Powers T, Seifert U (1995) Dynamical theory of the pearling instability in cylindrical vesicles. *Phys Rev Lett* 74:3384–3387.
20. Moroz JD, Nelson P, BarZiv R, Moses E (1997) Spontaneous expulsion of giant lipid vesicles induced by laser tweezers. *Phys Rev Lett* 78:386–389.
21. Ringsdorf H, Schlarb B, Venzmer J (1988) Molecular architecture and function of polymeric oriented systems—Models for the study of organization, surface recognition, and dynamics of biomembranes. *Angew Chem Int Ed Engl* 27:113–158.
22. Decher G, et al. (1989) Interaction of amphiphilic polymers with model membranes. *Angew Makromol Chem* 166:71–80.
23. Baumgart T, Hess ST, Webb WW (2003) Imaging coexisting fluid domains in biomembrane models coupling curvature and line tension. *Nature* 425:821–824.
24. Schulte MD, Rogers KL (2004) Thiols in hydrothermal solution: Standard partial molal properties and their role in the organic geochemistry of hydrothermal environments. *Geochim Cosmochim Acta* 68:1087–1097.

Supporting Information

Zhu et al. 10.1073/pnas.1203212109

SI Text

SI Materials and Methods. Fatty acids and fatty acid derivatives were obtained from Nu-Chek Prep (Elysian, MN). Fluorescent dyes were obtained from Invitrogen (Carlsbad, CA). Dithiothreitol, 3-mercaptopropionic acid, 3-mercapto-1-propanol, 1-mercapto-2-propanol, and 3-mercapto-1,2,4-triazole were purchased from Sigma-Aldrich (St. Louis, MO). Oleate vesicles were prepared by resuspending a dried film of oleic acid in 0.2 M Na-bicine (Sigma-Aldrich, St. Louis, MO) containing 2 mM HPTS at pH 8.5, to a final concentration of 10 mM oleic acid. The vesicle suspension was vortexed briefly and then tumbled overnight. Dilutions of vesicles were made using buffers containing fatty acids above the critical aggregate concentration (cac; approximately 80 μM for oleic acid), to avoid vesicle dissolution. Large (approximately 4 μm in diameter) monodisperse multilamellar vesicles were prepared by extrusion and large-pore dialysis as described (1). Briefly, extrusion of polydisperse vesicles through 5-μm-diameter pores eliminates vesicles larger than 5 μm in diameter. Dialysis of extruded vesicles against 3-μm-pore-size polycarbonate membranes then eliminates vesicles smaller than 3 μm in diameter, leaving behind a roughly monodisperse population of vesicles with a mean diameter of approximately 4 μm. Oleate vesicles in 0.2 M glycinamide hydrochloride were prepared and dialyzed using the same method. Oleate vesicles containing 1-hydroxypyrene (Sigma-Aldrich, St. Louis, MO) in the membrane were prepared by co-dissolving 1-hydroxypyrene (20 mol%), oleic acid, and Rh-DHPE (1 mol%) in a chloroform solution, followed by rotary evaporation and resuspension in buffer (0.2 M Na-bicine, pH 8.5, 15 mM DTT). Oleate vesicles containing di-L-cysteine were prepared by resuspension of 10 mM oleic acid in 0.2 M Na-bicine (pH 8.5) containing 2 mM HPTS and 20 mM di-L-cysteine. Di-L-cysteine (cysteinylcysteine) was prepared using F-moc solid phase synthesis on a microwave peptide synthesizer as described (2).

The methods for studying vesicle growth have been previously described (3). In the current study, vesicle growth experiments were performed in a buffer solution containing DTT, 3-mercaptopropionic acid, 3-mercapto-1-propanol, 1-mercapto-2-propanol, 3-mercapto-1,2,4-triazole, or di-L-cysteine. To prepare fatty acid micelle solutions for vesicle growth, fatty acids were dissolved in one equivalent of NaOH (final pH > 10), vortexed briefly, and agitated overnight under argon (4). Large (approximately 4 μm in diameter) multilamellar oleate vesicles (containing 2 mM HPTS) were prepared by large-pore dialysis, diluted 1:10 with the same buffer containing 0.8 mM oleic acid (to a final concentration of approximately 1 mM oleic acid), and stored in a microcentrifuge tube. To observe vesicle growth, five equivalents of oleate micelles were added to pre-formed vesicles, mixed, and then quickly pipetted into a disposable hemocytometer (Incyto, South Korea). The addition of smaller quantities (one equivalent) of oleate micelles was performed using the same method. Vesicles with encapsulated fluorescent dyes were imaged using a Nikon TE2000S inverted epifluorescence microscope with extra long working distance (ELWD) objective lenses (Nikon, Japan). The illumination source was a metal halide lamp (EXFO, Canada) with a 480 ± 20 nm (for HPTS), 546 ± 5 nm (for Rh-DHPE), or 360 ± 20 nm (for UV) optical filter (Chroma, Rockingham, VT). The illumination intensity was controlled using a set of two neutral density filters on the microscope. The images and movies were recorded using a digital camera (Hamamatsu Photonics, Japan) and post-processed using Phylum Live software (Improvision, Lexington, MA). All images were cropped using Photoshop CS4 (Adobe Systems, San Jose, CA), with linear adjustments of brightness and contrast.

All NMR spectra were recorded at 293 K with a Varian 400 MHz NMR spectrometer (Oxford AS-400) equipped with a 5 mm broadband PFG (z-gradient) probe. DTT and *trans*-4,5-dihydroxy-1,2-dithiane (Sigma-Aldrich, St. Louis, MO) at concentrations of 15–20 mM were added to sonicated vesicle suspensions prior to NMR measurements. Oleate vesicles were prepared without buffer by mixing 15 mM oleate with 7.5 mM NaOD (pH approximately 8.5, in 100% D_2O for STD experiments and in 10% D_2O for waterLOGSY experiments). All 1D STD spectra were recorded with 512 scans. Selective saturation of the vinyl protons of oleic acid hydrophobic chain at 5.3 ppm was performed by applying a series of 40 Gaussian-shaped pulses (50 ms; 1 ms delay between pulses) for a total saturation time of 2.04 s. Subtraction of saturated spectra from off resonance spectra (−4 ppm) was performed by phase cycling. Suppression of vesicle signals was achieved by relaxation filtering prior to detection. Water suppression was achieved by the excitation sculpting method.

WaterLOGSY spectra were recorded with 512 scans. The first water selective 180° refocusing *reburp* pulse of 32 ms was generated from a Pbox of VNMRJ 2.1A. For solvent selection echo, two pulsed field gradients (PFGs) at a pulse length of 2.5 ms and pulse power of 2.5 G/cm were first applied. During the mixing time (1.2 s), a weak rectangular PFG with a power level of 0.02 G/cm was applied. Subsequently, a short gradient recovery time of 2 ms was applied. Water suppression was achieved with an excitation sculpting sequence. The two water selective 180° pulses for solvent suppression echo were applied for a 4.9 ms pulse length. The four PFGs for solvent suppression echo had a pulse length of 0.8 ms and strength of 12 G/cm, respectively. Data were collected with the proton carrier set at 4.75 ppm, with a spectral width of 10,000 Hz, an acquisition time of 0.8 s, and a relaxation delay of 3.8 s. A T1ρ filter was applied to eliminate fast-relaxing vesicle signals.

1. Zhu TF, Szostak JW (2009) Preparation of large monodisperse vesicles. *PLoS ONE* 4:e5009.
2. Erdelyi M, Gogoll A (2002) Rapid microwave-assisted solid phase peptide synthesis. *Synthesis-Stuttgart*:1592–1596.
3. Zhu TF, Szostak JW (2009) Coupled growth and division of model protocell membranes. *J Am Chem Soc* 131:5705–5713.
4. Hanczyc MM, Fujikawa SM, Szostak JW (2003) Experimental models of primitive cellular compartments: Encapsulation, growth, and division. *Science* 302:618–622.

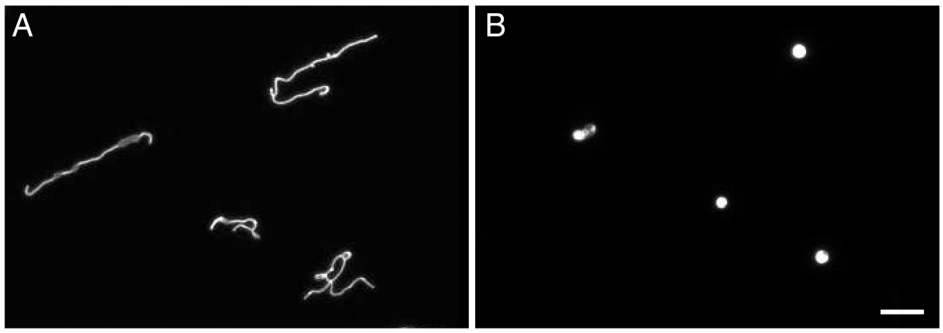

Fig. S1. Long thread-like oleate vesicles round up into large spherical vesicles. (*A*) Oleate vesicles (containing 2 mM HPTS, in 0.2 M Na-bicine, pH 8.5) 30 min after the addition of five equivalents of oleate micelles. (*B*) The long thread-like oleate vesicles rapidly (in approximately 5 s) round up into large spherical vesicles under intense illumination (Movie S1). Scale bar, 20 μm.

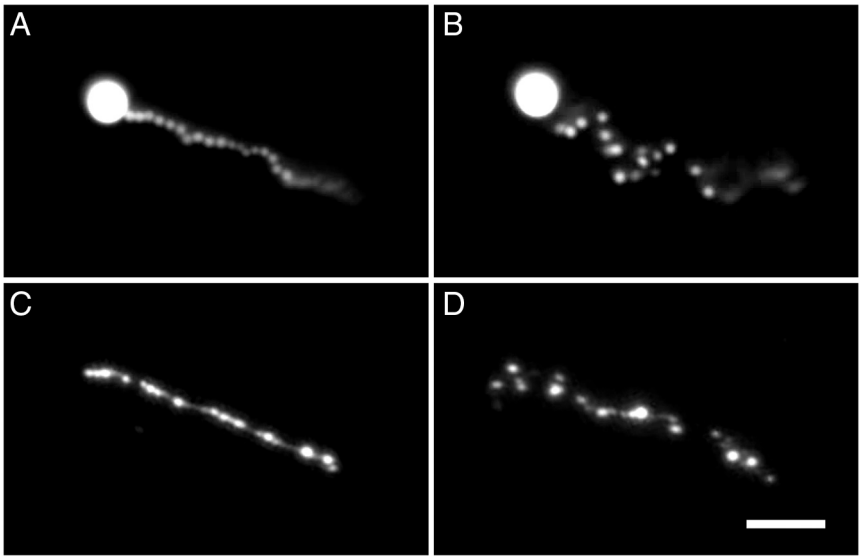

Fig. S2. Vesicle pearling and division under various conditions. (*A* and *B*) An oleate vesicle (containing 2 mM HPTS, in 0.2 M Na-bicine, pH 8.5, 10 mM DTT) 30 min after the addition of one equivalent of oleate micelles. Under intense illumination (for 2 s and 9 s, respectively), the filamentous portion of the vesicle went through pearling and division (Movie S3). (*C* and *D*) A decanoate:decanol (2:1) vesicle (in 0.2 M Na-bicine, pH 8.5, 30 min after the addition of two equivalents of decanoate micelles and one equivalent of decanol emulsion) went through pearling and division under intense illumination (for 3 s and 10 s, respectively). Scale bar, 10 μm.

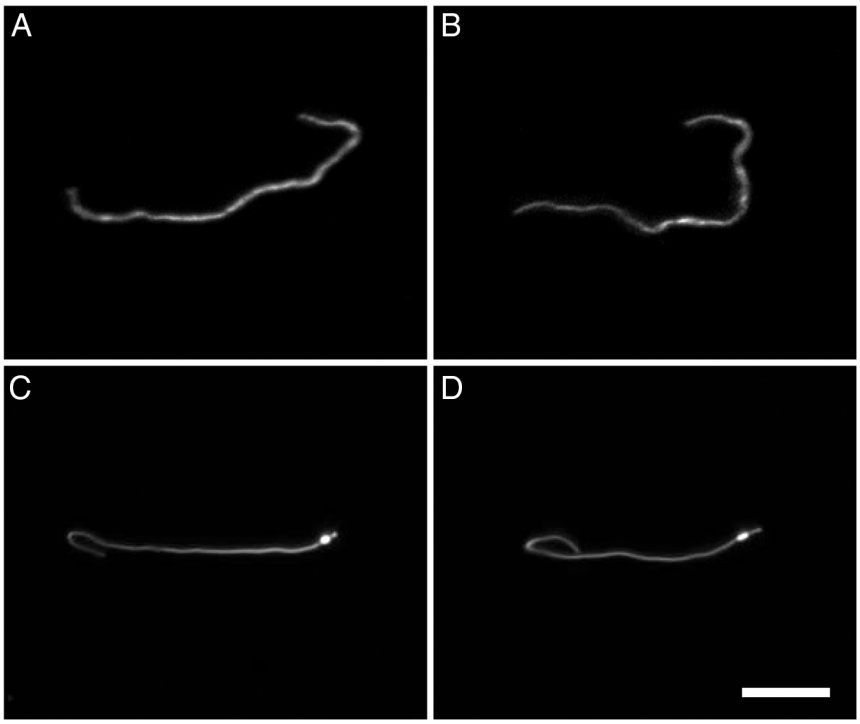

Fig. S3. Rh-DHPE labeled oleate vesicles and HPTS labeled POPC vesicles. (*A* and *B*) A long thread-like oleate vesicle labeled with a membrane-localized dye (0.5 mol% Rh-DHPE, in 0.2 M Na-bicine, pH 8.5, 10 mM DTT, 30 min after the addition of five equivalents of oleate micelles), under intense illumination for 10 s, did not go through pearling and division. (*C* and *D*) A long thread-like POPC vesicle (containing 2 mM HPTS, in 0.2 M Na-bicine, 0.5 M sucrose, pH 8.5, 10 mM DTT), under intense illumination for 10 s, did not go through pearling and division. Scale bar, 20 μm.

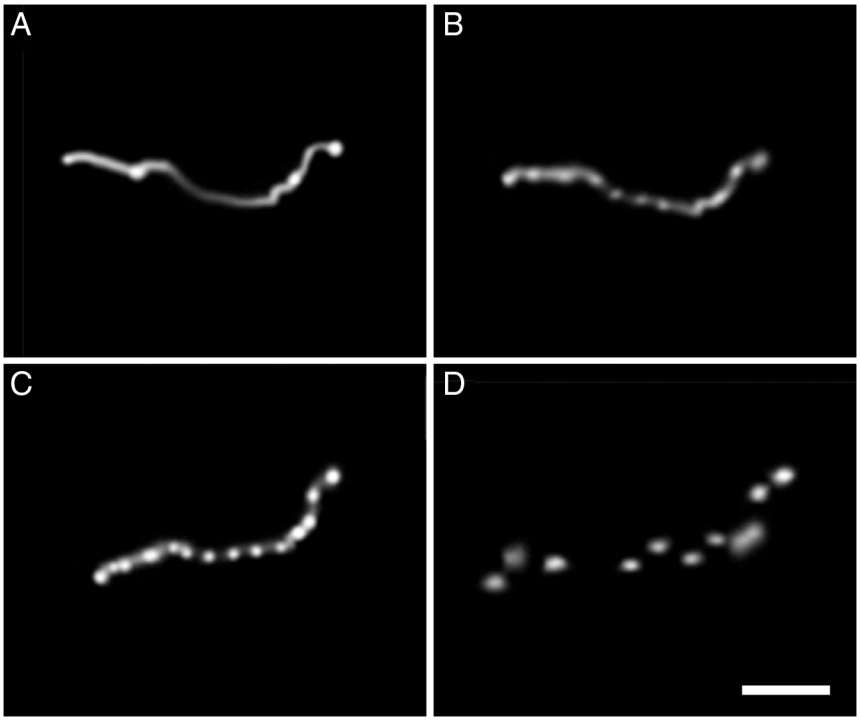

Fig. S4. Vesicle pearling and division with equal concentrations of HPTS inside and outside the vesicles. (*A*) An oleate vesicle with 2 mM HPTS inside and outside the membranes (labeled by 1 mol% Rh-DHPE for imaging, in 0.2 M Na-bicine, pH 8.5, 10 mM DTT) 30 min after the addition of five equivalents of oleate micelles. (*B–D*) Under intense illumination (for 2 s, 7 s, and 11 s, respectively), the long thread-like vesicle went through pearling and division. Scale bar, 10 μm.

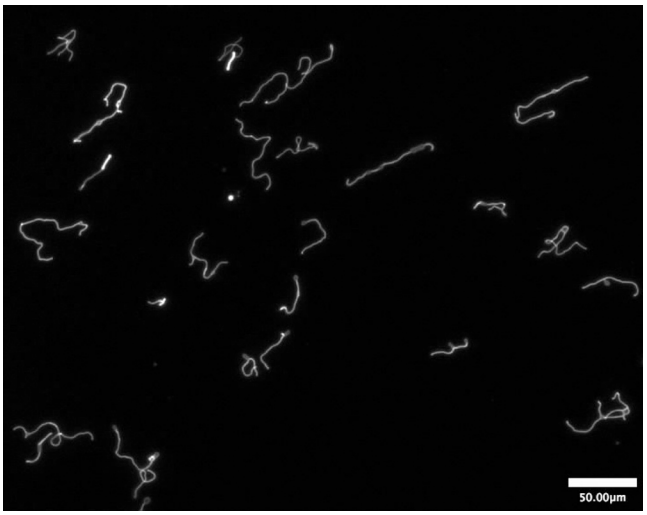

Movie S1. This real-time movie shows that long thread-like oleate vesicles (containing 2 mM HPTS, in 0.2 M Na-bicine, pH 8.5, 30 min after the addition of five equivalents of oleate micelles) rapidly (in approximately 5 s) round up into large spherical vesicles under intense illumination (QuickTime; 9 FPS; 7 MB). Scale bar, 50 μm.

Movie S1 (MOV)

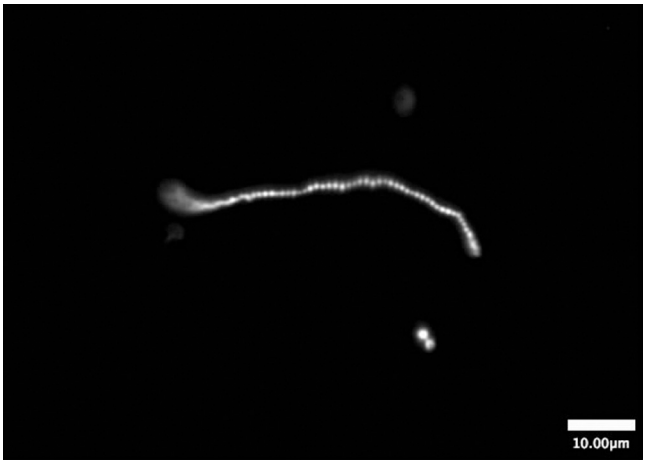

Movie S2. This real-time movie shows that a long thread-like oleate vesicle (containing 2 mM HPTS, in 0.2 M Na-glycinamide, pH 8.5, 10 mM DTT, 30 min after the addition of five equivalents of oleate micelles) went through pearling and division under intense illumination (QuickTime; 9 FPS; 2 MB). Scale bar, 10 μm.

Movie S2 (MOV)

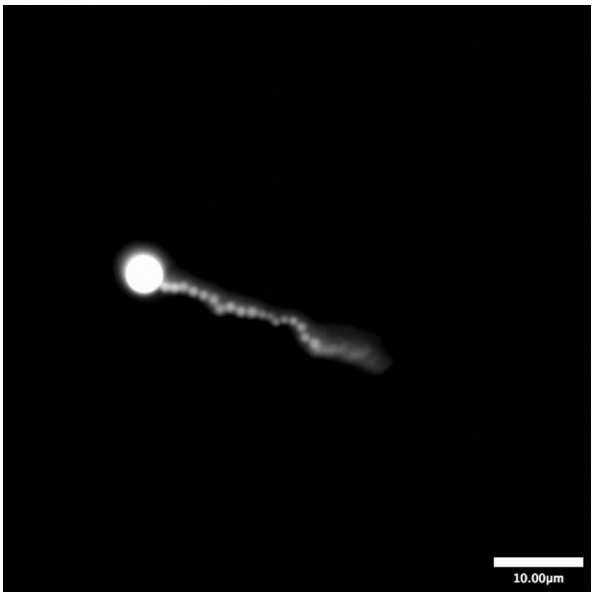

Movie S3. This real-time movie shows that the filamentous portion of an oleate vesicle (containing 2 mM HPTS, in 0.2 M Na-bicine, pH 8.5, 10 mM DTT, 30 min after the addition of one equivalent of oleate micelles), under intense illumination, went through pearling and division (QuickTime; 9 FPS; 1 MB). Scale bar, 10 μm.

Movie S3 (MOV)

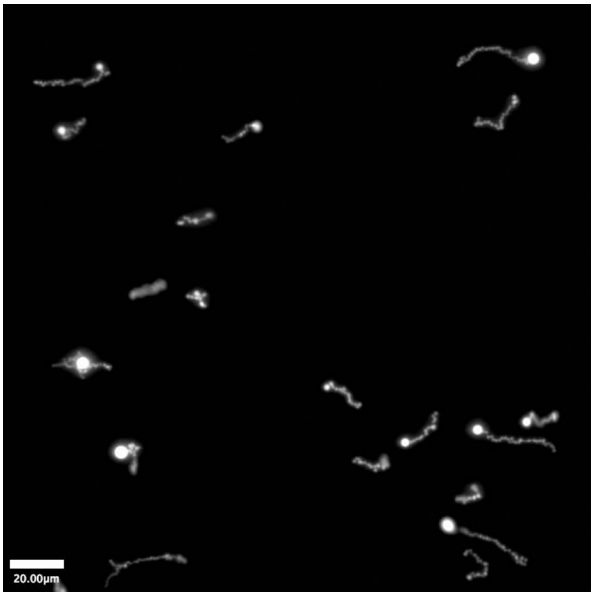

Movie S4. This real-time movie shows that the filamentous portions of a group of oleate vesicles (containing 2 mM HPTS, in 0.2 M Na-bicine, pH 8.5, 10 mM DTT, 30 min after the addition of one equivalent of oleate micelles), under intense illumination, went through pearling and division (QuickTime; 9 FPS; 5 MB). Scale bar, 20 μm.

Movie S4 (MOV)

Movie S5. This movie shows that a filamentous oleate vesicle (with 20 mol% 1-hydroxypyrene and 1 mol% Rh-DHPE in the membrane, in 0.2 M Na-bicine, pH 8.5, 15 mM DTT, 30 min after the addition of five equivalents of oleate micelles), under intense illumination, went through pearling and division (AVI; 25 FPS, 60X accelerated, timer on top shows mm:ss; 4 MB). Scale bar, 10 μm.

Movie S5 (AVI)